July 1998 ● NREL/CP-520-25045

Structure of Ge(100) Surfaces for High-Efficiency Photovoltaic Applications

J.M. Olson and W.E. McMahon

Presented at the 2nd World Conference and Exhibition on
Photovoltaic Solar Energy Conversion; 6-10 July 1998; Vienna, Austria

National Renewable Energy Laboratory
1617 Cole Boulevard
Golden, Colorado 80401-3393
A national laboratory of the
U.S. Department of Energy
Managed by the Midwest Research Institute
For the U.S. Department of Energy
Under Contract No. DE-AC36-83CH10093

STRUCTURE OF Ge(100) SURFACES FOR HIGH-EFFICIENCY PHOTOVOLTAIC APPLICATIONS

J.M. Olson and W.E. McMahon
National Renewable Energy Laboratory
Golden, CO 80401 USA

ABSTRACT: While much is known about the Ge(100) surface in a UHV/MBE environment, little has been published about this surface in an MOCVD environment. The main objective of this study is to determine the structure of the surface of Ge substrates in the typical MOCVD reactor immediately prior to and following the heteronucleation of GaAs and other lattice-matched III-V alloys, and to determine the conditions necessary for the growth of device-quality epilayers. In this paper we present the **first** STM images of the MOCVD-prepared Ge surfaces. Although many of the observed features are very similar to UHV- or MBE-prepared surfaces, there are distinct and important differences. For example, while the As-terminated surfaces for MBE-Ge and MOCVD-Ge are virtually identical, the AsH_3-treated surfaces in an MOCVD reactor are quite different. The terrace reconstruction is rotated by $\pi/2$, and significant step bunching or faceting is also observed. Time-dependent RD kinetic studies also reveal, for the first time, several interesting features: the transition rate from an As-terminated (1x2) terrace reconstruction to a stable AsH_3-annealed surface is a function of the substrate temperature, substrate miscut from (100) and AsH_3 partial pressure, and, for typical prenucleation conditions, is relatively slow. These results explain many of the empirically derived nucleation conditions that have been devised by numerous groups.

1. INTRODUCTION

Single-junction GaAs and GaInP/GaAs tandem solar cells are currently being produced using metal organic chemical vapor deposition (MOCVD) on a large scale for communication-satellite power applications. Virtually all of these devices are grown on Ge(100) substrates. Although there are a number of "recipes" for the growth of GaAs on Ge(100) with specular morphologies or low antiphase-domain (APD) or low stacking-fault densities, many present contradictory results. For example, Pelosi et al. [1] find that the GaAs surface morphology is best for very low V/III ratio (on the order of 1), using a moderate growth rate (Rg~3.5 µm/hr) and low growth temperature (Tg=600°C). On the other hand, Li et al. [2] find the lowest APD density occurs for high V/III, low Rg and high Tg. Chen et al. [3] showed that “good” morphology could only be obtained for growth temperatures in a range of 600°C to 630°C.

Heretofore, most of the basic studies of the surface of Ge(100) were conducted on samples prepared under ultrahigh vacuum (UHV) or molecular beam epitaxy (MBE) conditions (see reference [4]). Virtually no attention has been paid to MOCVD-prepared surfaces due to the lack of tools required to determine the nature of these surfaces. And although double-stepped, single-domain vicinal (100) surfaces are, from MBE studies, considered important for APD-free growth, little attention is paid to this aspect of the problem in most of the MOCVD papers.

The objective of this study is to determine some of the basic properties of Ge(100) surface prepared in a typical MOCVD environment using reflectance difference (RD) spectroscopy, scanning tunneling microscopy (STM), low energy electron diffraction (LEED), and Auger electron spectroscopy (AES).

2. EXPERIMENTAL

The general experimental setup is shown in Fig. 1. The STM, LEED, and AES are housed in a UHV chamber that is attached to the MOCVD reactor via a UHV transfer line. An MOCVD-prepared sample can be quickly quenched and transferred to the analytical chamber without exposing the surface to air or any other reactive atmosphere. Attached to the same transfer line is a solid-source III-V MBE reactor.

The RD spectrometer is attached to the MOCVD reactor as shown in Fig. 2 and is used to determine *in situ* the state of the surface in real time. This spectrometer measures

$$\frac{\Delta R}{R} = \frac{R_{\bar{1}10} - R_{110}}{\left(R_{\bar{1}10} + R_{110}\right)/2}, \qquad (1)$$

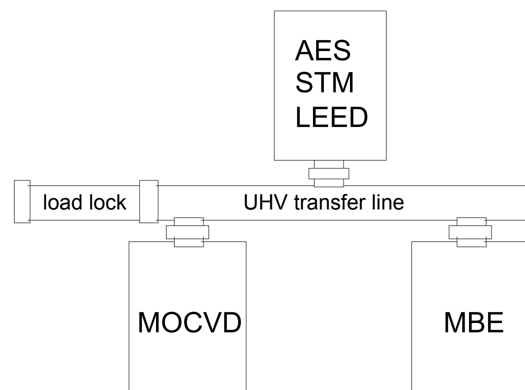

Figure 1. Schematic of MOCVD/MBE/Surface Analysis Cluster Tool.

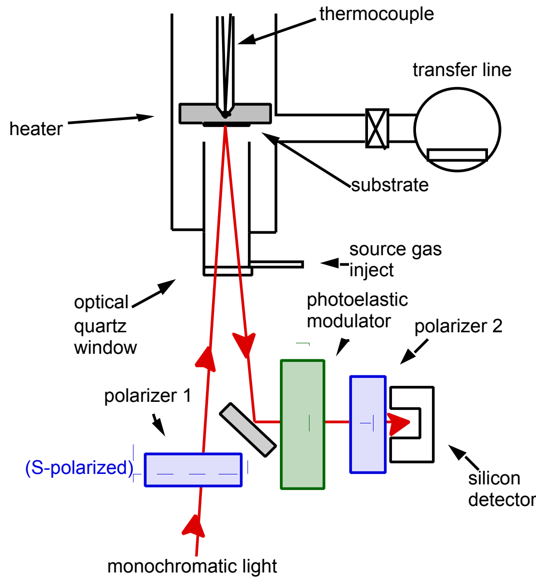

Figure 2. Schematic of RDS/MOCVD setup.

where $R_{\bar{1}10}$ and R_{110} are the reflectances for light polarized in the as-noted crystallographic direction. Further details are published elsewhere [5, 6].

The wafers were cleaned using a method similar to that described by Fitzgerald et al. [7]. The wafers were first etched in $1NH_4OH{:}1H_2O_2{:}10H_2O$ at room temperature for 1 min. This removes about 0.2 µm. The wafer is then rinsed in deionized H_2O for 2 min followed by 1 min in $1HCl{:}1H_2O_2{:}10H_2O$ and a 2-min rinse in flowing DI H_2O. The wafers are then blown dry with a stream of N_2 gas. The HCl-based solution also etches Ge at 0.2 µm/min. The samples are then spin-dried and mounted on molybdenum carriers. The carriers are heated radiatively with a low thermal mass resistance heater. The temperature of the sample is determined by optical pyrometry. The MOCVD reactor pressure was fixed at 70 torr with a H_2 carrier flow of 6 slm.

From a surface science point of view, the hot interior surfaces of a typical MOCVD reactor are an infinite source of impurities. Our reactors are used routinely to grow III-V compounds of Ga, In, Al, As, and P. Hence, if the last material grown in the reactor is, for example, GaInP, a subsequent anneal of Ge(100) in this reactor will contaminate the surface with, primarily, P and In. Therefore, the results in section 3.1. were achieved using a freshly cleaned reactor. For section 3.2., we used clean molybdenum susceptors in a GaAs-contaminated reactor. This contamination yields a finite partial pressure of As upstream of the substrate.

After annealing, the samples are quenched to room temperature and transferred quickly to the analytical chamber. The quench rate is between 200 and 300°C/min and the total transfer time is less than 10 min.

The STM images were recorded at a sample bias of –3 V and a tunneling current of 1 nA. With the exception of tilting and artificial illumination to enhance the contrast, the STM are as recorded.

3. RESULTS

All the Ge(100) surfaces examined in this study exhibited a 1x2 or 2x1 reconstruction to some degree. Schematics of these two reconstructions are presented in Fig. 3. The arsenic-free Ge(100) and As:Ge(100) results are very similar to those found for UHV- or MBE-prepared surfaces. The Ge dimer bonds form a 2x1 array with the bond axis parallel to the [011] step edge. With the addition of As to this surface, the surface symmetry becomes 1x2, comprised of As dimers with bond axes perpendicular to the step edges. In the following, we will briefly show the results for the clean Ge(100) and As:Ge(100) phases, then compare and contrast with the results for samples annealed in AsH_3.

3.1 Clean Ge(100)

The two principal contaminants of most Ge surfaces are carbon and oxygen. Exposing the surface to H_2 at elevated temperatures readily removes oxygen. The free energy for the reaction

$$GeO_2 + 2H_2 \Leftrightarrow Ge + 2H_2O \qquad (2)$$

goes through zero at about 500 K [8]. Hence at typical growth temperatures, there is virtually no germanium oxide on the surface of the growing crystal and indeed none is found with AES after annealing in H_2.

Prolonged annealing times in H_2 at elevated temperatures are required to remove C; the mechanism by which this occurs is not known. However, C is easily removed by annealing the sample in a partial pressure of AsH_3 or PH_3. Presumably, the atomic hydrogen from the dissociation reaction of the hydride molecule quickly reacts with the C contaminants to produce the stable, volatile species CH_4.

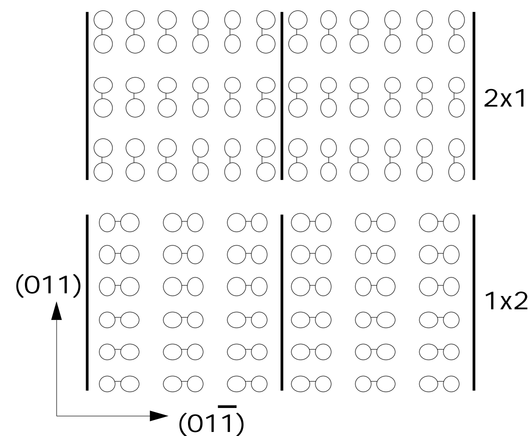

Figure 3. Summary of Ge(100) or As:Ge(100) surface phases. The Ge or As dimer bonds are represented by an array of dumbbells. For the 2x1 reconstruction, the dimer rows run perpendicular to the step edges (represented by thick vertical line segments). If the terrace reconstruction determines the GaAs sublattice orientation, then the 1x2 As:Ge(100) surface phase should produce GaAs with B-type (011) steps.

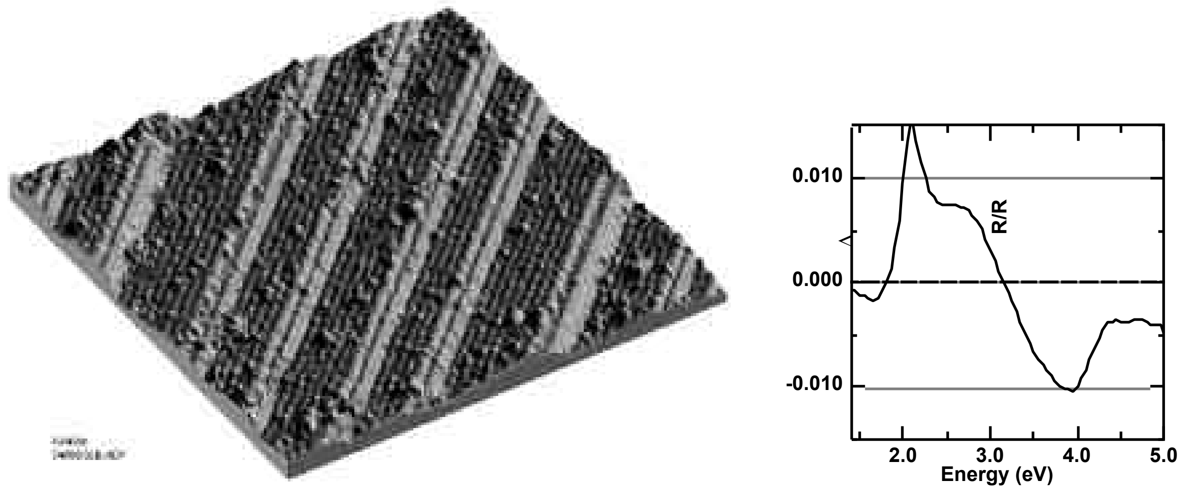

Figure 4. (a) STM image of As:Ge(100)6°(111). Dimer rows run parallel to step edges. (b) RD spectrum at room temperature for this surface.

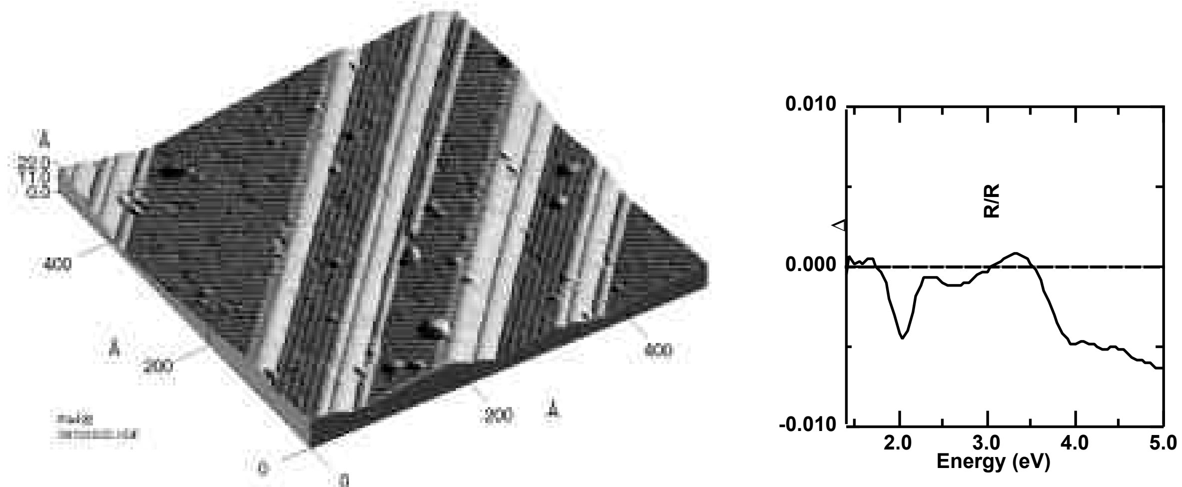

Figure 5. (a) STM image of a Ge(100)6°(111) surface annealed in AsH_3 at 640°C for 15 min. Surface is two-domain with dimer rows both parallel and perpendicular to the step edges. Steps are bunching to form facets. Step bunching process is facilitated by a slow AsH_3 etching of the Ge.

3.1.1. Low temperature Ge(100) phase

When clean, the surface of Ge(100) in UHV reconstructs, forming long rows of Ge-Ge dimers with a 2x1 surface reconstruction. Surfaces misoriented or tilted towards a [011] direction by a few degrees are composed of (100) terraces separated by steps that are $a_0/2$ high (where a_0=0.565 nm, the lattice constant of Ge) and the terrace width is $a_0/2/\tan\theta$ (where θ is the miscut angle from (100)). In a H_2 ambient, there is a tendency towards this state, but we find a higher surface concentration of the 1x2 surface reconstruction. This difference is probably not intrinsic to H_2, but is more likely due to the pinning of steps by impurities. We almost always see C on this surface with AES, and Gan et al. [9] have seen similar behavior.

The surface structure in real and reciprocal space was viewed with LEED and STM, respectively. The splitting of the [01] spots identifies the direction of the miscut and the average terrace width, and the half-order spots between the [11] and [01] normal spots indicate the direction of dimer-bond orientation.

The RD spectrum for this surface exhibits weak features around the critical points of bulk Ge, in particular, the critical point E_1 = 2.1 eV. This is indicative of a mixed 2x1/1x2 reconstructed surface and is consistent with the LEED and STM images.

3.1.2 High-temperature Ge(100) phase

At an annealing temperature greater than a critical temperature of about T_{cr} = 630°C, the RD spectrum is virtually featureless and samples quenched to room temperature exhibit a 1x1 LEED pattern with a high background. These results suggest that above 630°C, the Ge(100) surface becomes atomically rough.

3.2. As:Ge(100)

An STM image of the As:Ge(100) surface is shown in Fig. 4. Annealing the sample, in the absence of AsH_3, in an As-contaminated MOCVD reactor generates this surface. Arsenic, from warm reactor parts upstream of the substrate, reacts with the surface of Ge, breaking the Ge-Ge dimers and reforming an orthogonal array of As-As dimers. This STM image and a LEED pattern for this surface show a single domain, 1x2 reconstruction, and an ordered step array indicative of a step height of a_0. The RD spectrum for this surface (as shown in Fig. 4b) now exhibits a strong positive peak at or near E_1 and a negative peak around E_2.

At annealing temperatures less than T_{cr}, the intensity of the E_1 peak decreases with increasing temperature. Above T_{cr}, the RD spectrum is again featureless. However, in contrast to clean Ge(100), we were not able to quench this surface. As the temperature falls below T_{cr} during the quench, the 1x2 RD spectrum quickly re-emerges. The LEED for this sample is a poorly formed 1x2 pattern and AES shows the presence of As at the monolayer concentration.

3.3. AsH_3:Ge(100)

Arsine has a very unexpected effect on the surface of Ge. We first found that it slowly etches Ge. At an annealing temperature of 540°C and an AsH_3 partial pressure of 0.12 torr, the rate is ~0.5 ML/s. If Ge(100)6°(111) is annealed in AsH_3, the surface converts to a state characterized by the STM image shown in Fig. 5. This surface is two-domain with dimer rows running both parallel and perpendicular to the step edges. The terraces are wider and the steps higher than those in the STM micrograph of Fig. 4 for As:Ge(100), indicating the formation of step bunching and microfaceting. LEED images of the surface confirm the step bunching and show that the reconstruction is predominantly 2x1 with a minority 1x2 component.

The RD peak near E_1 has a flipped sign and is typically less intense than its As:Ge(100) counterpart. The rate of change of E_1 depends on AsH_3 partial pressure and temperature, as shown in Fig. 6. Note the long time constants associated with the AsH_3 annealing/etching. The steady state intensity of the E_1 peak decreases with increasing temperature, presumably because of changes in the relative populations of 2x1 and 1x2 domains on the surface. Also, in contrast to the clean Ge(100) and the As:Ge(100) phases, the RD spectrum is relatively stable above T_{cr}.

If the AsH_3 partial pressure in the reactor is reduced to zero, the surface converts reversibly to a state determined by the annealing temperature and the condition of the reactor and substrate holder. Above T_{cr}, the RD spectrum quickly approaches flat line. Below T_{cr}, with a GaAs-free substrate holder, the RD spectrum slowly evolves into the 1x2 spectrum; for a GaAs-coated substrate holder, the RD spectrum is close to flat line. This anomalous state is the focus of our current efforts.

We also examined a number of other (100) miscuts, and the results for the "verboten" miscut towards (110) is shown in Fig. 7. This surface is constructed of both 1x2 and 2x1 terraces with two orthogonal (11n)-like risers. The high quality image of Fig. 7 clearly portrays the complex step-riser reconstructions that can occur on miscut AsH_3:Ge(100) surfaces.

4. DISCUSSION

Ge(100) substrates annealed in AsH_3 exhibit surface phases that differ significantly from As:Ge(100) and clean Ge(100) annealed under UHV conditions. The main cause for this unexpected behavior is probably due to the fact that arsine etches Ge. At equilibrium, in the absence of growth or etching, it is expected that a single domain, 1x2 or 2x1 reconstruction, should prevail. This is driven mainly by the step-edge-terrace interaction energies. If a monolayer of Ge (or As) is added to or removed from this surface, the dimer orientation must rotate by 90°. If the AsH_3 etches the surface in monolayer increments, the local surface symmetry must alternately switch between 1x2 and 2x1 as etching proceeds. And if the surface is quenched at some instance, we would expect to see a mixed domain surface.

The development of microfacets is probably also the result of AsH_3 etching. In general, the fastest etching surfaces prevail (the opposite of growth). Step bunching can be caused by kinetic anisotropies associated with the etching process or can also be affected by step and terrace energies variations caused by reactions with other species such as AsH_3.

The net effect of etching is to yield a surface that is

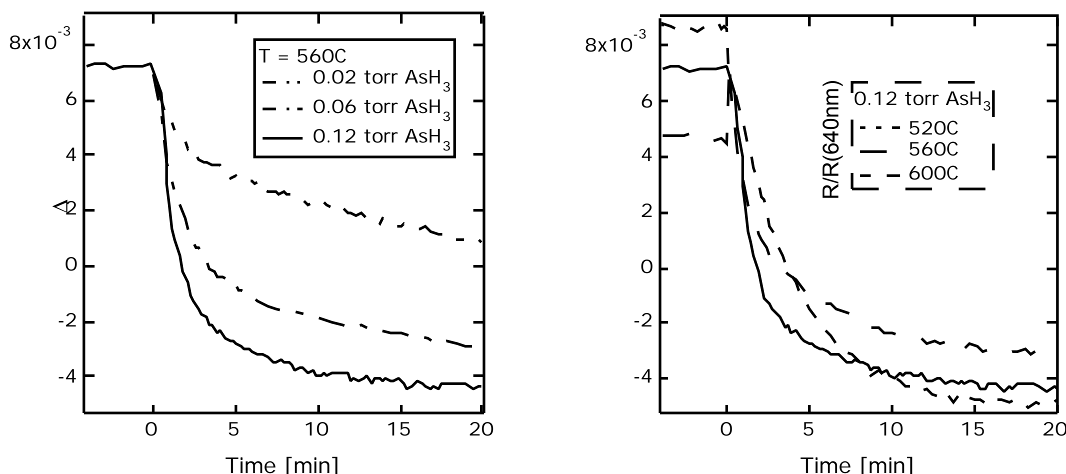

Figure 6. Transient RD signal at E_1 for a series of AsH_3 partial pressures and annealing temperature. The initial state is 1x2 As:Ge(100).

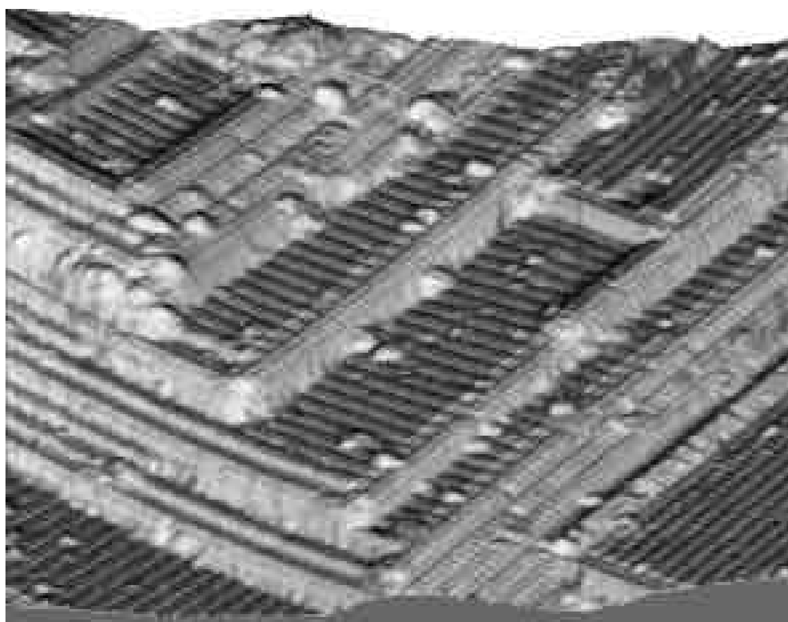

Figure 7. STM image of Ge(100)6°(110) annealed in AsH_3 at 640°C and an arsine partial pressure of 0.12 torr. Both 2x1 and 1x2 terraces are present. Individual terrace dimers and individual facet atoms are clearly visible. Microfacets show clear evidence of reconstruction.

Figure 8. TEM micrograph showing antiphase domains (small truncated triangles) at the GaAs/Ge interface. The Ge(100)6°(111) substrate was annealed in AsH_3 under conditions similar to those use in Fig. 5.

probably less than ideal for the subsequent heteroepitaxy of GaAs. If the state of the surface just before growth is similar to Fig. 5, we might expect to see antiphase domains and a relatively rough interface. In Fig. 8, we show a transmission electron microscopy (TEM) micrograph of a GaAs layer grown on Ge(100)6°(111) similar to that in Fig. 5. It shows the presence of APDs as bright, rounded, or truncated triangular regions at the GaAs/Ge interface. These are eventually overgrown by the dominant domain. Although they do not extend far into the epilayer, they do appear to spawn other defects. A high-resolution TEM micrograph of the interface shows that the interface is indeed rough on an atomic level with a scale similar to that in Fig. 5.

These results also emphasize the importance of pregrowth conditions. It is quite clear that pregrowth parameters such as AsH_3 partial pressure, annealing

temperature and time, and reactor history and design may be more important than the particular reactor conditions during nucleation and growth. For example, it is customary to introduce arsine into the reactor at or near the beginning of a growth run. The time constant associated with the arsine/Ge etching reaction depends strongly on the arsine partial pressure. The prenucleation heatup and soak times relative to this etching time constant are now important parameters, because they probably determine the state of the surface immediately prior to nucleation.

5. SUMMARY AND CONCLUSIONS

Ge(100) substrates annealed in AsH_3 exhibit surface phases that differ significantly from As:Ge(100) and clean Ge(100) annealed under UHV conditions. We found that arsine etches Ge and precludes the development of a single-domain surface. It also causes step bunching and faceting.

Better devices and higher production yields may result from careful manipulation of the pregrowth conditions such as AsH_3 partial pressure, annealing temperature and time, and reactor history and design.

Contradictory results in the literature may be due to variations of the pregrowth conditions, which, in most cases, are not well documented.

ACKNOWLEDGMENTS

We wish to thank Sarah Kurtz, D.J. Friedman, and J. Geisz for useful discussions. We would also like to thank K. Jones and M.M. Al-Jassim for the TEM micrographs. The work was sponsored by the U. S. Department of Energy, Office of Energy Research, Basic Energy Sciences, Division of Materials Science and by the U. S. Department of Energy under contract number DE-AC36-83CH10093.

REFERENCES

[1] C. Pelosi, G. Attolini, C. Bocchi, P. Franzosi, C. Frigeri, M. Berti, A. V. Drigo, and F. Romanato, “The role of the V/III ratio in the growth and structural properties of metalorganic vapor phase epitaxy GaAs/Ge heterostructures,” *J Electron Mater*, **24**, 1723-1730 (1995).

[2] Y. Li, G. Salviati, M. M. G. Bongers, L. Lazzarini, L. Nasi, and L. J. Giling, “On the formation of antiphase domains in the system of GaAs on Ge,” *J Cryst Growth*, **163**, 195-202 (1996).

[3] J. C. Chen, M. L. Ristow, J. I. Cubbage, and J. G. Werthen, “GaAs/Ge Heterojunction Grown by Metal-Organic Chemical Vapor Deposition and Its Application to High Efficiency Photovoltaic Devices,” *J Electron Mater*, **21**, 347-353 (1992).

[4] T. Yasuda, L. Mantese, U. Rossow, and D. E. Aspnes, “Surface-induced optical anisotropies of single-domain (2 x 1) reconstructed (001) Si and Ge surfaces,” *Phys Rev Lett*, **74**, 3431-3434 (1995).

[5] J. S. Luo, J. M. Olson, S. R. Kurtz, D. J. Arent, K. A. Bertness, M. E. Raikh, and E. V. Tsiper, “Optical anisotropy and spontaneous ordering in Ga0.5In0.5P: An investigation using reflectance-difference spectroscopy,” *Phys Rev B-Condensed Matter*, **51**, 7603-7612 (1995).

[6] J. S. Luo, J. F. Geisz, J. M. Olson, and M. C. Wu, “Surface-related optical anisotropy of GaInP, InP, and GaP,” *J Cryst Growth*, **174**, 558-563 (1997).

[7] E. A. Fitzgerald, J. M. Kuo, Y. H. Xie, and P. J. Silverman, “Necessity of Ga Prelayers in GaAs/Ge Growth Using Gas-Source Molecular Beam Epitaxy,” *Appl Phys Lett*, **64**, 733-735 (1994).

[8] T. B. Reed, *Free Energy of Formation of Binary Compounds*. Cambridge: The MIT Press, 1971.

[9] S. Gan, L. Li, T. Nguyen, H. Qi, R. F. Hicks, and M. Yang, “Scanning tunneling microscopy of chemically cleaned germanium (100) surfaces,” *Surface Sci*, **395**, 69-74 (1998).